

RSC Advances



This is an *Accepted Manuscript*, which has been through the Royal Society of Chemistry peer review process and has been accepted for publication.

Accepted Manuscripts are published online shortly after acceptance, before technical editing, formatting and proof reading. Using this free service, authors can make their results available to the community, in citable form, before we publish the edited article. This *Accepted Manuscript* will be replaced by the edited, formatted and paginated article as soon as this is available.

You can find more information about *Accepted Manuscripts* in the [Information for Authors](#).

Please note that technical editing may introduce minor changes to the text and/or graphics, which may alter content. The journal's standard [Terms & Conditions](#) and the [Ethical guidelines](#) still apply. In no event shall the Royal Society of Chemistry be held responsible for any errors or omissions in this *Accepted Manuscript* or any consequences arising from the use of any information it contains.



Journal Name

ARTICLE

Tertiary butyl hydroquinone as a novel additive for SEI film formation in lithium-ion batteries

Jia-Qi Liu,^{a,†} Quan-Chao Zhuang,^{a,†} Yue-Li Shi,^{a,b,*} Xiaodong Yan,^b Xing Zhao,^a Xiaobo Chen^{b,*}

Received 00th January 20xx,
Accepted 00th January 20xx

DOI: 10.1039/x0xx00000x

www.rsc.org/

Electrolyte additives play a key role in the performance of the lithium ion batteries. In this study, we reported tertiary butyl hydroquinone (TBHQ) as a new electrolyte additive with a promising prospect. It largely improved the electrochemical performance of the graphite electrode such as cyclic stability and reversible capacity. The improvement was benefited from the effective formation of a stable and compact thin solid-electrolyte-interface (SEI) film to reduce the resistance. Thus, this study demonstrated a promising electrolyte additive for improving lithium-ion battery performance.

Introduction

Currently, graphite is the most widely used anode material in commercially available lithium-ion batteries due to its relatively high theoretical capacity (372 mAh g⁻¹), low potential, moderate cost and environmental benignity.¹ LiPF₆-containing mixture solvents of organic carbonates are commonly used as electrolytes for lithium-ion batteries, where organic carbonates generally include ethylene carbonate (EC), diethyl carbonate (DEC), dimethyl carbonate (DMC), and ethylmethyl carbonate (EMC). It is generally known that during the first intercalation of lithium into the graphite electrode, part of electrolyte would be reduced to form a surface film on graphite electrode, well known as the solid electrolyte interface (SEI) film. The SEI film is the key to the reversible intercalation/deintercalation of Li⁺ into/from graphite that occurs at a potential far beyond the stability limits of nonaqueous electrolytes.² Initially, the SEI film protects the electrode against further electrolyte decomposition at large negative voltage and the exfoliation of the graphite. But the formation of the SEI film results in an irreversible loss of capacity on the initial charge-discharge cycle of the lithium-ion batteries, and gradual capacity fading may occur as the SEI layer thickens over time.³ A compact and stable film is believed to improve the stability and rate performances of the carbon electrodes.⁴ Generally, the properties of the SEI film depend strongly on the electrolyte composition. The use of additives to the electrolytes is one of the most efficient methods to alter

the properties of the SEI films on the surface of the anodes.⁵⁻⁷

Based on their functions and reaction mechanisms, electrolyte additives can be divided into reduction-type additives and reaction-type additives.⁸ For reduction-type additives, the reduction potential is higher than that of the electrolyte, that is, the electrochemical reduction reaction of the additives occurs before the electrolyte decomposes. This results in a protective solid film on the surface of the electrode and thus is able to suppress the decomposition of electrolyte. These additives play important roles in both reducing gas generation and increasing the stability of the SEI film through the participation of additive molecular moieties into the SEI film. vinylene carbonate (VC)⁹, fluoroethylene carbonate (FEC)¹⁰ and vinyl ethylene carbonate (VEC)¹¹ are typical reduction-type additives widely used in commercial lithium ion batteries. For reaction-type additives, in the potential range of lithium ion intercalation, they may not be reduced electrochemically, however they can help to form more desired SEI film through either scavenging radical anions, forming intermediate compounds with the solvent reduction, or reacting with subsidiary products of the electrolyte decomposition such as lithium alkyl dicarbonate and lithium alkyloxy. For example, dialkylpyrocarbonate, an in situ CO₂-provider^{12,13} through the degradation reaction, is a typical reaction-type additive. Other typical reaction-type additives include carboxyl phenol, aromatic esters¹⁴, and anhydride¹⁵ with well-conjugated structures to stabilize intermediate radical anions by delocalization of the radical, maleic anhydride,¹⁶ succinimide and N-benzyloxycarbonyloxy succinimide¹⁷ where "N" atom is linked by two carbonyl groups with strong radical anion-delocalizing ability. Compared with reduction-type additives, the study of the reaction-type additives is still in their infancy.

^a Lithium-ion Batteries Laboratory, School of Materials Science and Engineering, China University of Mining and Technology, Xuzhou 221116, China. Yue-Li Shi, Tel: +8613852081106, E-mail: zwysyl@163.com.

^b Department of Chemistry, University of Missouri – Kansas City (UMKC) Kansas City, MO 64110, USA. Xiaobo Chen, Tel: +18162356420, E-mail: Email: chenxiaobo@umkc.edu.

† These authors contributed equally to this work (co-first authors).

Electronic Supplementary Information (ESI) available: [details of any supplementary information available should be included here]. See DOI: 10.1039/x0xx00000x

Here, we reported the use of TBHQ as a reaction-type additive to electrolyte for lithium-ion batteries. Tertiary butylhydroquinone (TBHQ), an aromatic organic compound, is a derivative of hydroquinone, substituted with a tert-butyl group. It has been commonly used as a synthetic food antioxidant to prevent oils and fats from oxidative deterioration and rancidity.¹⁸ It is a highly effective antioxidant by reacting with radicals, namely, a radical-scavenging compound.¹⁹ Moreover, it is cheap, non-toxic, lipophilic and dissolves easily in common electrolytes.²⁰⁻²² In this study, the typical electrolyte 1.0 M LiPF₆-EC:DMC:DEC (1:1:1, v/v/v) was used to study the effect of TBHQ on the electrochemical properties of the graphite electrode. Charge-discharge, cyclic voltammetry (CV), and electrochemical impedance spectroscopy (EIS) were used to analyze the electrochemical processes. The results showed that the introduction of TBHQ could effectively improve the capacity and cyclic stability of the graphite electrode by forming a thin, uniform, compact and smooth SEI film.

Results & Discussion

Figure 1 showed the first-cycle CV curves recorded on the graphite electrodes in the electrolyte with and without the TBHQ additive. In the electrolyte without the TBHQ additive, there were three reductive current peaks: peak I at 0.8 V, peak II at 0.5 V, and peak III near 0 V, corresponding to the reduction of EC into Li₂CO₃ (a single electron reduction process), the reduction of EC into alkyl lithium carbonate (a double electrons reduction process), and the intercalation of lithium ions into the graphite electrode, respectively.^{23,24} In the electrolyte with TBHQ, peaks I and II related to EC reduction process remain almost unchanged, along with the unchanged peak III. As no other current peaks were observed, TBHQ was electrochemically stable in the entire potential range of lithium ion intercalation.

The first-cycle charge/discharge curves of the graphite electrodes in electrolytes without and with TBHQ were displayed in Figure 2A. The charge capacities of the graphite electrodes in electrolytes without and with TBHQ were 442 mAh·g⁻¹ and 415 mAh·g⁻¹, respectively. Apparently, TBHQ

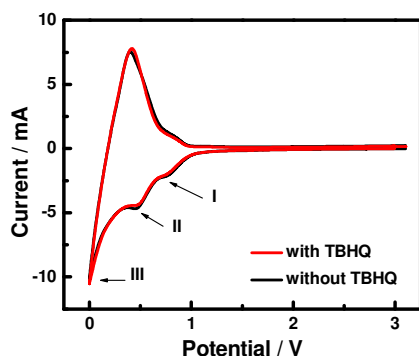


Figure 1. Initial CV curves of graphite electrodes in 1.0 M LiPF₆-EC:DMC:DEC electrolyte with and without TBHQ.

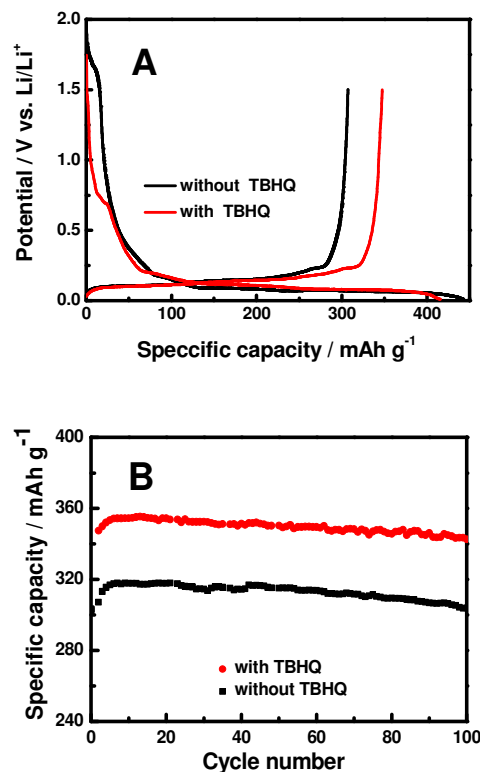


Figure 2. (A) Charge-discharge characteristics of graphite electrode in the electrolytes without and with TBHQ. (B) Cyclic discharge performances of graphite electrodes in 1.0 M LiPF₆-EC:DMC:DEC (1:1:1, v/v/v) electrolyte without and with TBHQ.

increased the charge capacity of the graphite electrode. However, the discharge capacities of the graphite electrodes in electrolytes without and with TBHQ were 307.2 mAh·g⁻¹ and 347.5 mAh·g⁻¹, respectively. Thus, TBHQ enhanced the discharge capacity of the graphite electrode. The irreversible capacities were 135 mAh·g⁻¹ and 68 mAh·g⁻¹, for the electrolytes without and with TBHQ, respectively. Introducing TBHQ in the electrolyte obviously reduced the irreversible capacity and improved the faradic efficiency of the graphite electrode.

The cyclic discharge performance was shown in Figure 2B. In the electrolyte without the TBHQ additive, the discharge capacity of the graphite electrode increased gradually from 307.2 to 317.8 mAh·g⁻¹ at the 10th cycle, and then decreased to 303.4 mAh·g⁻¹ after 100 cycles. The capacity retention was 98.8% relative to the first cycle. When the graphite electrode cycled in the electrolyte with TBHQ, the discharge capacity increased from 347.5 mAh·g⁻¹ to 355.3 mAh·g⁻¹ at the 12th cycle, and then decreased to 342.6 mAh·g⁻¹ after 100 cycles. The capacity retention was 98.6% compared to the first cycle. Therefore, adding TBHQ in the electrolyte obviously increased the cyclic discharge performance (342.6 mAh·g⁻¹ vs. 303.4 mAh·g⁻¹) with a 12.9% capacity enhancement after 100 cycles.

Figure 3 showed the Nyquist plots of the graphite electrodes at various potentials from 1.2 to 0.2 V in the first discharge process. For both electrolytes with and without TBHQ, at the potential large than 0.9 V (Figure 3A), there were a small semicircle in the high-frequency region (high-frequency semicircle, abbreviated as HFS) and a large arc in the low-frequency region. When the potential drops to 0.9 V (Figure 3B-D), the Nyquist plots consisted of three parts, namely HFS, middle-frequency semicircle (MFS) and an inclined line in the low frequency (low frequency line, LFL). According to the study by D. Aurbach, HFS, MFS and LFL are attributed to the lithium diffusion across the SEI film covering on the graphite electrode, charge transfer process, and the solid-state diffusion of the lithium-ion in the graphite matrix, respectively.²⁵⁻²⁷

The HFS was observed at a rather high potential (3.0 V, and Figure S1). A previous study by Change and Sohn indicated that graphite promoted decomposition of electrolyte and formation of SEI film without an applied potential.²⁸ In the study by Little, it was proposed that the HFS was likely caused by contact resistance between the graphite electrode and the current collector.²⁹ Hence, the HFS might be associated not only with the Li^+ migration through the SEI film, but also with contact resistance between the graphite electrode and the current collector.

In order to reveal the underlying mechanism, an equivalent circuit shown in Figure 4A was used to explain the Nyquist plots in Figure 3. In this equivalent circuit, R_s represents the ohmic resistance, while R_{SEI} and R_{ct} are resistances of the SEI film and the charge transfer reaction. Q_{SEI} and Q_{dl} represent the capacitances of the SEI film and the double layer, respectively. The capacitances of the SEI film and the double layer are represented using the constant phase elements (CPE) Q_{SEI} and Q_{dl} , respectively. Considering the fact that the low frequency region cannot be

modelled properly using the finite Warburg element, we use a CPE instead, i.e. Q_D which is related to lithium ion solid-state diffusion

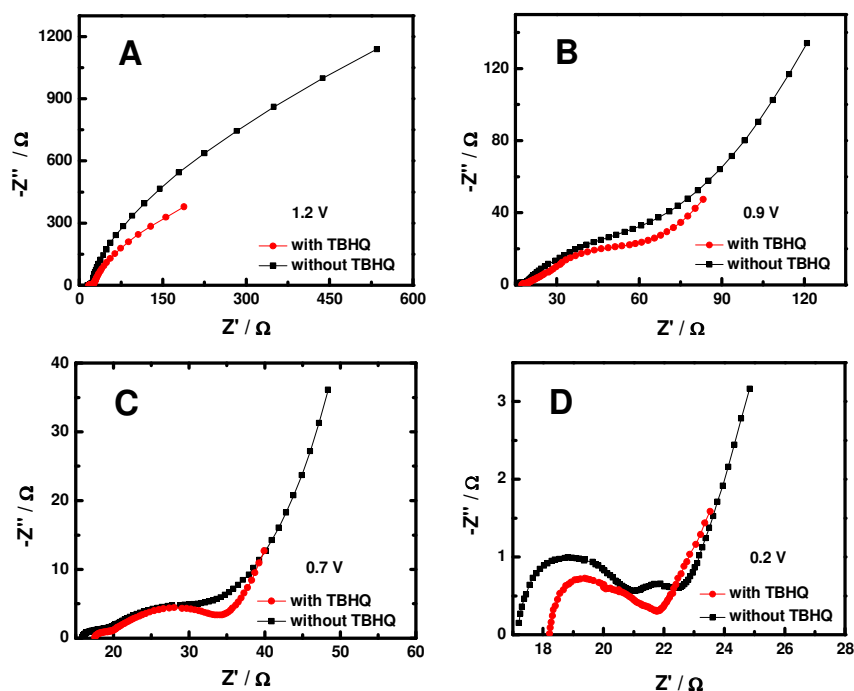


Figure 3. Nyquist plots of the graphite electrodes in the first discharge process in the 1.0 MLiPF₆-EC: DMC: DEC (1:1:1, v/v/v) electrolyte without and with TBHQ at various potentials: (A) 1.2 V, (B) 0.9 V, (C) 0.7 V, and (D) 0.2 V.

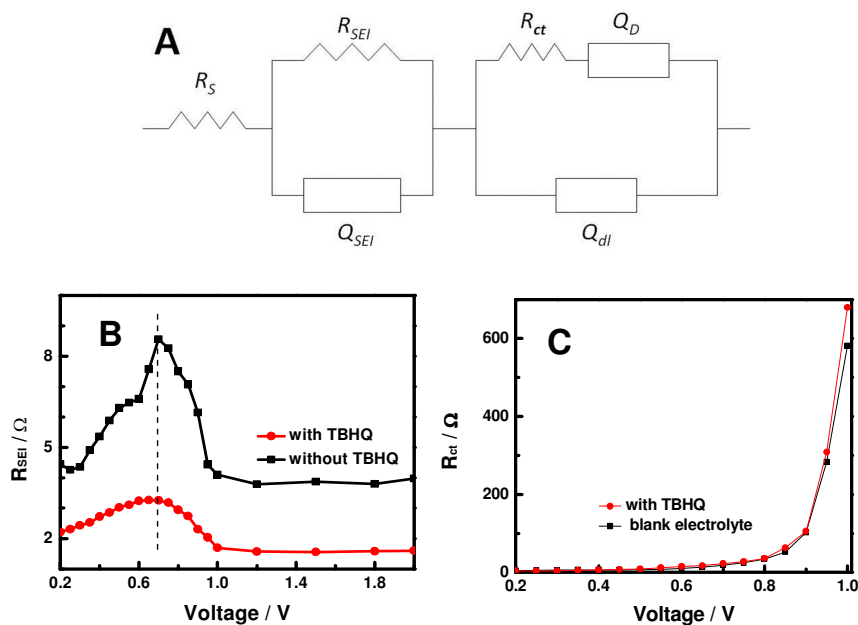


Figure 4. (A) Equivalent circuit proposed for fitting impedance spectra of the graphite electrodes, R_s is the ohmic resistance, R_{SEI} and R_{ct} are resistances of the SEI film and the charge transfer reaction. Q_{SEI} and Q_{dl} represent the capacitances of the SEI film and the double layer. Variations of R_{SEI} (B) and R_{ct} (C) with the electrode potential in electrolytes without and with TBHQ.

in the graphite electrode. This method has been successfully used to characterize the graphite electrodes. The CPE describes the non-ideal behavior of the composite electrode (porosity of the material, roughness of the surface), and is fit for simulating the graphite electrode.³⁰⁻³⁶ The equivalent electrical circuit simulated impedance spectrum were compared with experimental EIS data at 0.7 V and 0.2 V in the discharge process in Figure S3 and the parameter values were listed in Table S1 and Table S2. The relative standard deviation for most fitted parameters did not exceed 15%. Therefore, the proposed equivalent circuit can satisfactorily describe the experimental data.

The changes of R_{SEI} were shown in Figure 4B. For the electrolyte without TBHQ, R_{SEI} remained almost unchanged in the potential range 3.0–1.2 V. From 1.0 V to 0.7 V, R_{SEI} increased rapidly owing to the formation of the SEI film. When the electrode potential decreased from 0.7 V to 0.2 V, R_{SEI} decreased rapidly, likely due to that the reduction products of EC, for example, alkyl lithium carbonate reacted with the trace amount of water to form a composition with higher lithium ion conductivity.^{37,38} The change trend of R_{SEI} in electrolytes with TBHQ was similar to that of R_{SEI} in electrolyte without TBHQ. R_{SEI} in electrolytes with TBHQ remained almost unchanged in the potential range 3.0–1.2 V. From 1.0 V to 0.65 V, R_{SEI} increased rapidly. From 0.65 V to 0.2 V, R_{SEI} decreased rapidly.

However, the value of R_{SEI} with TBHQ electrolytes was smaller than that of R_{SEI} without TBHQ electrolytes. $R_{SEI} = \rho/lS$, where l is the thickness of the SEI film, S the electrode surface area, ρ the resistivity. The resistivity of SEI film formed in electrolytes with and without TBHQ are a little different. In the experiments, the surface areas of the graphite electrodes are same. So, it is clear that the change of the resistance R_1 reflects the change of the thickness of the SEI film. Therefore, smaller value of R_{SEI} with TBHQ electrolytes indicates that adding TBHQ in the pristine electrolyte might favor a thinner SEI film on graphite electrode. Figure 4C showed the variations of R_{ct} with the electrode polarization potential in the electrolyte without and with TBHQ. The existence of TBHQ had negligible effect on the charge-transfer resistance R_{ct} .

The expression for the admittance response of the CPE (Q) is

$$Y = Y_0 \omega^n \cos\left(\frac{n\pi}{2}\right) + j Y_0 \omega^n \sin\left(\frac{n\pi}{2}\right)$$

where ω is the angular frequency, j the imaginary unit. A CPE represents a resistor when $n = 0$, a capacitor with capacitance of C when $n = 1$, an inductor when $n = -1$, and a Warburg resistance when $n = 0.5$. In this study, Y_0 is considered to be a pseudo capacitance (pseudo- Y_0) when n lies between 0.5 and 1.^{39,40} The value of n gives the degree of distortion of the impedance spectra and when $n=1$, Y is identical to C_i and the CPE becomes an ideal capacitor. Larger values of n between 0.5 and 1 indicate the properties of the pseudo capacitance are more close to an ideal capacitance. The surface of the pseudo capacitance are more uniform.^{41,42}

For the electrolyte without TBHQ, Q_{SEI-n} increased slowly from 1.0 V to 0.65 V (from 0.67 to 0.81) (Fig. S4.), reached the maximum at 0.65 V, then remained almost unchanged from

0.65 V to 0.2 V (from 0.81 to 0.76) after the potential of the SEI film formed (consistent with Fig. 4B). The value of n in the electrolyte without TBHQ changed between 0.67 and 0.76, indicating Q_{SEI} was a pseudo capacitance. Q_{SEI-n} in the electrolyte with TBHQ increased quickly from 0.9 V to 0.65 V (from 0.3 to 0.81) and increased slowly from 0.65 V to 0.2 V (from 0.81 to 0.93) after the SEI film formation (consistent with Fig. 4B). Q_{SEI-n} in the electrolyte with TBHQ was larger than that in the electrolyte without TBHQ after the SEI film formation below 0.65 V, indicating that the properties of Q_{SEI} were closer to an ideal capacitance and uniformity of the SEI film was improved.

Q_{SEI-Y} (Fig. S5.) for the electrolyte without and with TBHQ decreased quickly from 1.0 V to 0.65 V and changed a little from 0.65 V to 0.2 V. Q_{SEI-Y} in the electrolyte with TBHQ was smaller than that in the electrolyte without TBHQ after the SEI film formation below 0.65 V. The above results showed that TBHQ introduction in the electrolyte led to form a more homogenous SEI film with lower capacitance value.

The change of Q_{dl-n} and Q_{dl-Y} in electrolytes without and with TBHQ were shown in Fig. S6. and Fig. S7. Q_{dl-n} in electrolytes without and with TBHQ decreased with the electrode potential decreasing. Q_{dl-n} in electrolytes with TBHQ was from 0.66 to 0.57 at 0.75 V - 0.2 V, which was higher than that in electrolytes without TBHQ (from 0.60 to 0.48). While Q_{dl-Y} in electrolytes with TBHQ was lower than that in electrolytes without TBHQ from 0.75 V to 0.2 V. Q_{dl-Y} varied very little among the range of 0.01 F to 0.06 F.

Q_D-n and Q_D-Y in electrolytes without and with TBHQ were shown in Fig. S8 and Fig. S9. Q_D-n decreased with the electrode potential decreasing from 0.8 V to 0.2 V. Q_D-n in electrolytes with TBHQ was lower than that in electrolytes without TBHQ from 0.8 V to 0.2 V. Q_D-Y in electrolytes with TBHQ was higher than that in electrolytes without TBHQ.

The morphologies of the graphite electrodes after CV test in the electrolytes with and without TBHQ were shown in Figure 5. The surface of the graphite electrode in the electrolyte without TBHQ had some obvious defects and large grain sizes (Figures 5A and 5B). The surface of the graphite electrode after CV measurement in the electrolyte with TBHQ was smoother and more compact (Figures 5C and 5D). This indicated that the addition of TBHQ helped the formation of a better SEI film.

According to the studies of Endo et al.^{43,44}, the initial reaction in the electrochemical reduction of the electrolyte involves electron transfer from the cathodically polarized electrode to the solvent molecules, and the process coordinates with the lithium cation to produce a radical anion of the solvent. This achieves electron transfer equilibrium with the neighboring solvent molecules coordinated with the same lithium cation. The subsequent decomposition will be initiated from this equilibrium. Thus, if the initial reaction in the reductive decomposition of electrolyte solutions can be affected, the performance of lithium-ion and lithium secondary batteries may be improved.

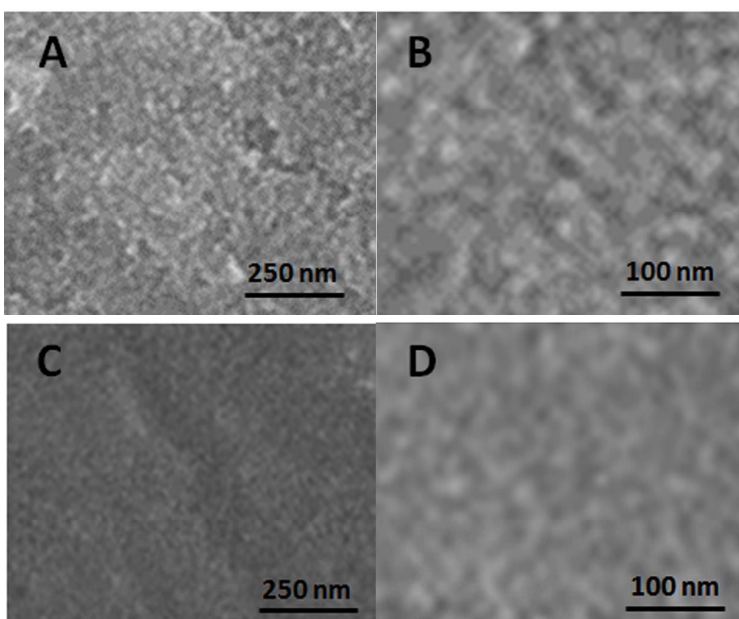
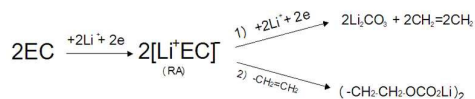


Figure 5. SEM images of the graphite electrodes after CV measurement in the electrolytes without (A, B) and with (C, D) TBHQ.

Two mechanisms have been proposed for the electrochemically induced reduction of EC^{45-48} , as shown below.



Radical anions are abbreviated as RAs. Both mechanisms are present in the process of SEI film formation and compete with each other. When mechanism (I) (corresponding to peak I in CV) is predominant, the reduction of solvents generates more gaseous products, and the resulting SEI film is Li_2CO_3 -abundant and less stable. On the contrary, mechanism (II) (corresponding to peak II in

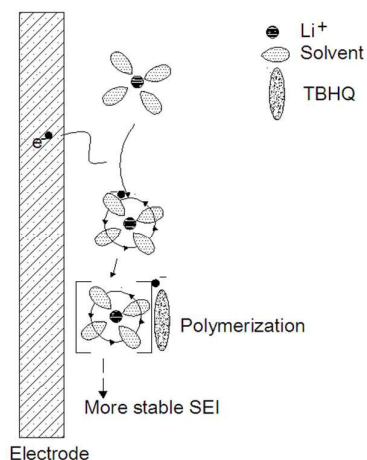


Figure 6. A proposed model for the reaction mechanism of TBHQ.

CV) leads to less gaseous products and the resulting products are substantially insoluble in the electrolyte. As a result, the generated SEI film is more compact and smooth. TBHQ is a highly effective anti-oxidant and has a well-conjugated structure⁴⁹⁻⁵¹. It is believed to be able to capture less stable radical anions through delocalization of the radical, and to form a polymer with the $[Li^+EC]^-$ through capture radical anions. The polymerization will decompose to form a new product, eventually form a thin, uniform, compact and smooth SEI⁵²⁻⁵⁵.

The reaction mechanism of TBHQ as a SEI film formation additive for lithium ion batteries was proposed as shown in Figure 6: (i) electron transfer occurring from the cathodically polarized electrode to the solvent molecule coordinated with the lithium cation to produce a radical anion; (ii) electron transfer equilibrium with the neighboring solvent molecules coordinated with the same lithium cation; (iii) TBHQ capturing less stable radical anions to form a polymer with the $[Li^+EC]^-$; (iiii) the reductive decomposition of the polymerization to form a more thin, uniform, compact and smooth SEI film and reduced gas generation in the first intercalation of Lithium ions into graphite. The SEI film, such interphases, situating between electrode surfaces and electrolyte, is formed by sacrificial electrolyte decomposition and consuming a certain amount of lithium ion during the initial charging, and constitutes a barrier to allow ionic conduction and forbid electronic conduction.⁵⁶ Introducing TBHQ in electrolytes could favor a thin, uniform, compact and smooth SEI film on graphite electrode. A thinner SEI film can reduce the resistance of SEI and reduce the molecular decomposition EC. So formation of a thinner SEI film can consume less electrolyte and lithium ion during the initial charging. Thus the irreversible capacity is reduced and the faradic efficiency is improved during the first-cycle charge/discharge process. The uniform, compact and smooth SEI film has better mechanical properties with increasing the flexibility, which can prevent the SEI rupture caused by insertion and extraction of lithium ions. The stable SEI film can prevent further reaction between electrode surfaces and electrolyte⁵⁷⁻⁶⁰. Thus a stable SEI layer is beneficial to the cyclic performances.

Conclusions

TBHQ was demonstrated as a new and stable additive for lithium ion batteries. The electrochemical performance of graphite electrode such as cyclic stability and reversible capacity was improved in the electrolyte with TBHQ, due to the formation of a thin, uniform, compact and smooth SEI layer.

Experimental

The graphite electrodes were prepared by spreading a mixture of 90% Micro-carbon fiber (MCF) (Petoca, Japan) and 10% polyvinylidene fluoride (PVDF) (HSV910, USA) binder dissolved in N-methyl-2-pyrrolidone (NMP, Alfa Aesar) onto a piece of copper foil (thickness: 0.025mm) current collector. The solvent and the water were removed by baking at 80 °C in the air and 120 °C in vacuum, respectively, and the dried electrodes were suppressed by a roller at room temperature to obtain a smooth and compact structure. The pristine electrolyte was 1.0 M LiPF₆ in a mixture of EC, DMC and DEC (1:1:1, volume ratio, Tianci Co., Guangzhou, China). 0.1 wt% TBHQ was added into the pristine electrolyte as the additive.

Charge-discharge test was evaluated through the CR2032-type coin cell. Coin cells were assembled with graphite as the working electrode and lithium as the foil counter electrode, polypropylene microporous separator (Celgard 2400) soaked in the electrolyte as the separator. The coin cells were galvanostatically charged and discharged in a battery analyzer (Neware, Shenzhen, China) over a range of 1.5-0.001 V vs. Li/Li⁺ at a constant current density of 0.1C (1C=372 mA g⁻¹).

CV and EIS were carried out in a three-electrode glass cell with Li foils as the counter and reference electrode on an electrochemical workstation (CHI660C, Chenhua Co., Shanghai, China) at room temperature. The area of the work electrode was 1.5×1.5 cm². CV was measured in the potential range from 3 V to 0 V at a scan rate of 1 mV·s⁻¹. EIS was measured in the frequency range from 10⁵ to 10⁻² Hz with the potentiostatic signal amplitude of 5 mV and the frequency range from 10⁵ to 10⁻² Hz. The electrode was equilibrated for 1 h before the EIS measurements to attain steady-state conditions. The impedance results obtained were fitted using Zview software. The specimen after CV test was transferred into the glove box and washed in DMC and dried in vacuum to remove the residual electrolyte. The morphology of the graphite electrode after electrochemical tests in different electrolyte compositions was investigated by a LEO 1530 Field Emission Scanning Electron Microscopy (FE-SEM, Oxford Instrument).

Acknowledgements

Y. Shi appreciates the support from China Scholarship Council and China University of Mining and technology. X. C. thanks the support from the College of Arts and Science, University of Missouri – Kansas City.

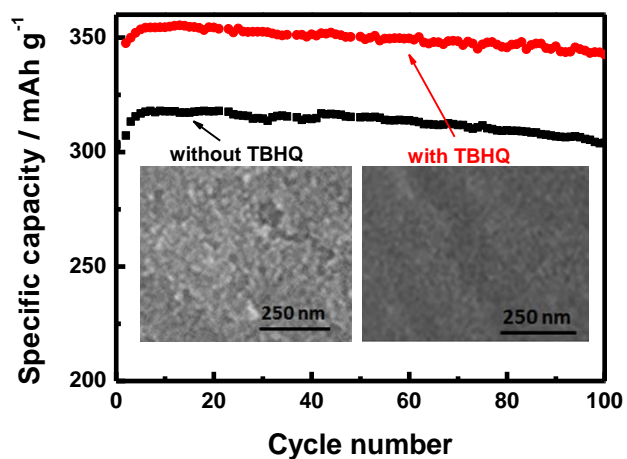
Notes and references

- 1 B. Moradi and G. G. Botte, *J Appl. Electrochem*, 2016, **46**, 123.
- 2 Y. He, M. Liu, Z.D. Huang, B. Zhang, Y. Yu, B.H. Li, F.Y. Kang and J. K. Kim, *J. Power Sources*, 2013, **239**, 269.
- 3 Y.X. Lin, Z. Liu, K. Leung, L.Q. Chen, P. Lu and Yue Qi, *J. Power Sources*, 2016, **309**, 221.
- 4 S.Y. Li, X.L. Xu, X.M. Shi, B.C. Li, Y.Y. Zhao, H.M. Zhang, Y.L. Li, W. Zhao, X.L. Cui and L.P. Mao, *J. Power Sources*, 2012, **217**, 503.

- 5 G. Gourdin, J. Collins, D. Zheng, M. Foster and D. Qu, *Electrochem. Soc.* 2015, **1**, 118.
- 6 J. C. Burns, A. Kassam, N. N. Sinha, L. E. Downie, L. Solnickova, B. M. Wayand J. R. Dahn, *J. Electrochem. Soc.*, 2013, **160**, A1451.
- 7 S.Y. Jung, H.S. Kim, J.G. Lee, J.H. Ryu and S. M. Oh, *J. Electrochem. Soc.*, 2016, **163**, 2, A223.
- 8 D. Aurbach, J.S. Gnanaraj, W. Geissler and M. Schmidt, *J. Electrochem. Soc.*, 2004, **151**, A23.
- 9 L. Liao, X. Cheng, Y. Ma, P. Zuo, W. Fang, G. Yin and Y. Gao, *Electrochim. Acta*, 2013, **87**, 466.
- 10 H. Shin, J. Park, A. M. Sastry and W. Lu, *J. Electrochem. Soc.* 2015, **162**, A1683.
- 11 S.D. Xu, Q.C. Zhuang, J. Wang, Y.Q. Xu and Y.B. Zhu, *Int. J. Electrochem. Sci.*, 2013, **8**, 8058.
- 12 M.D. Levi, E. Markevich, C. Wang, M. Koltypin and D. Aurbach, *J. Electrochem. Soc.*, 2004, **151**, A848.
- 13 J.T. Lee, M.S. Wu, F.M. Wang, Y.W. Lin, M.Y. Bai and P.C. Chiang, *J. Electrochem. Soc.*, 2005, **152**, A1837.
- 14 C. Wang, H. Nakamura, H. Komatsu, M. Yoshio and H. Yoshitake, *J. Power Sources*, 1998, **74**, 142.
- 15 J. Ufheil, M.C. Baertsch, A. Wursig and P. Novak, *Electrochim. Acta*, 2005, **50**, 1733.
- 16 J.H. Ku, S.S. Hwang, D.J. Ham, M.S. Song, J.K. Shon, S.M. Ji, J.M. Choi and S.G. Doo, *J. Power Sources*, 2015, **287**, 36.
- 17 N. Shahabadi, M. Maghsudi, Z. Kiani and M. Pourfoulad, *Food Chem.*, 2011, **124**, 1063.
- 18 S. Kashanian and J. Dolatabadi, *Food Chem*, 2009, **116**, 743.
- 19 C. Rockwell, V. Gangur, J. Pestka, R. Para, A. Turley, J. Zagorski, J. Bursley and H. Dover, *J. Immun.* 2014, **192**, 119.30.
- 20 Christinawaty, S. Damayanti, *Asian J Pharm Clin Res*, 2015, **8**, 4, 209.
- 21 S. S. Zhang, K. Xu and T. R. Jow, *J. Power Sources*, 2004, **130**, 281.
- 22 S. Rana, P. Sen and S.K. Bandyopadhyay, *Mater. Chem. Phys.* 2016, **169**, 173.
- 23 A. M. Haregewoin, E. G. Leggesse, J.C. Jiang, F.M. Wang, B.J. Hwang and S. D. Lin, *Electrochimica Acta*, 2014, **136**, 274.
- 24 D. Aurbach, M. D. Levi, E. Levi, H. Telier, B. Markovsky, G. Salitra, U. Heider and L. Hekier, *J. Electrochem. Soc.*, 1998, **145**, 3024.
- 25 D. Aurbach, *J. Power Sources*, 2000, **89**, 206.
- 26 M. D. Levi and D. Aurbach, *J. Phys. Chem. B*, 1997, **101**, 4630.
- 27 M. Holzapfel, A. Martinet, F. Alloin, B. Le Gorrec, R. Yazami and C. Montella, *J. Electroanal. Chem.*, 2003, **546**, 41.
- 28 Y. C. Chang and H. J. Sohn, *J. Electrochem. Soc.*, 2000, **147**, 50.
- 29 C. Wang, I. Kakwan, A. J. Appleby and F. E. Little, *J. Electroanal. Chem.*, 2000, **489**, 55.
- 30 Q.C. Zhuang, J. Li and L.L. Tian, *J. Power Sources*, 2013, **222**, 177.
- 31 M. L. Shi, *AC Impedance Spectroscopy Principles and Applications*, 2001, National Defense Industry Press, Beijing, 27.
- 32 Y. B. He, M. Liu, Z.D. Huang, B. Zhang, Y. Yu, B.H. Li, F. Kang and J.K. Kim, *J. Power Sources*, 2013, **239**, 269.
- 33 L.J. Yang, X.Q. Cheng, Y.L. Ma, S.F. Lou, Y.Z. Cui, T. Guan and G.P. Yin, *J. Electrochem. Soc.*, 2013, **160**, 11, A2093.
- 34 A. M. Haregewoin, E. G. Leggesse, J.C. Jiang, F.M. Wang, B.J. Hwang and S. D. Lin, *Electrochim. Acta.*, 2014, **136**, 274.
- 35 F. Yao, D. T. Pham and Y. H. Lee, *ChemSusChem*. 2015, **8**, 2284.
- 36 S. Carrara, V. Bavastrello, D. Ricci, E. Stura and C. Nicolini, *Sensors Actuators B*, 2005, **109**, 221.
- 37 A. M. Haregewoin, E. G. Leggesse, J.C. Jiang, F.M. Wang, B.J. Hwang and S. D. Lin, *Electrochim. Acta*, 2014, **136**, 274.
- 38 R. Bernhard, M. Metzger and H. A. Gasteiger, *J. Electrochem. Soc.* 2015, **162**, A1984.

- 39 Q.C. Zhuang, T. Wei, L.L. Du, Y.L. Cui, L. Fang and S.G. Sun, *J. Phys. Chem. C*, 2010, **114**, 8614.
- 40 Q.C. Zhuang, J. Li and L.L. Tian, *J. Power Sources*, 2013, **222**, 177.
- 41 K.M. Shaju, G.V. Subba Rao and B.V.R. Chowdari, *Electrochim. Acta*, 2003, **48**, 2691.
- 42 Q.C. Zhuang, Z.F. Chen, Q.F. Dong, Y.X. Jiang, L. Huang and S.G. Sun, *Chin. Sci. Bulletin*, 2006, **51**, 17.
- 43 Endo, K. Tanaka and K. Sekai, *J. Electrochem. Soc.*, 2000, **147**, 4029.
- 44 Y. Ein-Eli, S.F. McDevitt, D. Aurbach, B. Markovsky and A. Schechter, *J. Electrochem. Soc.*, 1997, **144**, L180.
- 45 D. Aurbach and Y. Ein-Eli, *J. Electrochem.*, 1995, **142**, 1746.
- 46 D. Aurbach, M. D. Levi, E. Levi and Alexander Schechter, *J. Phys. Chem. B.*, 1997, **101**, 2195-2206.
- 47 Y. Wang, S. Nakamura, M. Ue and P. B. Balbuena, *J. Am. Chem. Soc.*, 2001, **123**, 11708-11718.
- 48 T. Li, L. Xing, W. Li, Y. Wang, M. Xu, F. Gu, S. Hu, *Journal of Power Sources.*, 2013, **244**, 668-674.
- 49 J. Li, Y. Bi, W. Liu, S. Sun, C. Liu and S. Ma, *J Am Oil Chem Soc.*, 2014, **91**, 1763-1771.
- 50 A. Thomas, A. Vikraman, D. Thomas and Krishnapillai Girish Kumar, *Food Anal. Methods.*, 2015, **8**, 2028-2034.
- 51 A. Turley, J. Zagorski and C. Rockwell, *Cytokine*, 2015, **71**, 289-295.
- 52 I. A. Shkrob, Y. Zhu, T.W. Marin and D. Abraham, *J. Phys. Chem. C.*, 2013, **117**, 19270-19279.
- 53 K. Ushirogata, K. Sodeyama, Y. Okuno and Y. Tateyama, *J. Am. Chem. Soc.*, 2013, **135**, 11967-11974.
- 54 E.G. Leggesse and J.C. Jiang, *RSC Adv.*, 2012, **2**, 5439-5446.
- 55 Y. Wang, S. Nakamura, K. Tasaki and P.B. Balbuena, *J. AM. CHEM. SOC.*, 2002, **124**, 4408-4421.
- 56 L. Suo, O. Borodin, T. Gao, M. Olguin, J. Ho, X.I. Fan, C. Luo, C.s. Wang and K. Xu, *Science.*, 2015, 350(6263), 938-943.
- 57 K. Eom, J. Jung, J. Lee, V. Lair, T. Josh, S. Lee, Z. Lin and T. Fuller, *Nano Energy.*, 2015, **12**, 314-321.
- 58 B. Young, D. Heskett, C. Nguyen, M. Nie, J. Woicik and B. Lucht, *Appl. Mater. Interfaces.*, 2015, **7**, 20004-20011.
- 59 R. Schmitz, P. Murmann, R. Schmitz and I. Laskovic, *Progress in Solid State Chemistry*, 2014, **42**, 65-84.
- 60 J. Zheng, H. Zheng, R. Wang, L. Ben, W. Lu, L. Chen, L. Chen and H. Li, *Phys. Chem. Chem. Phys.*, 2014, **16**, 13229-13238.

TOC



Tertiary butyl hydroquinone (TBHQ), as a new electrolyte additive, largely improved the electrochemical performance of the graphite electrode (cyclic stability and reversible capacity), benefited from the formation of a stable and compact thin solid-electrolyte-interface (SEI) film.